



Published in final edited form as:

*J Am Chem Soc.* 2023 June 21; 145(24): 13059–13068. doi:10.1021/jacs.3c01347.

## Site Reversal in Nucleophilic Addition to 1,2,3-Triazine 1-Oxides

Luca De Angelis,

Graham C. Haug,

Gildardo Rivera,

Soumen Biswas,

Ammar Al-Sayyed,

Hadi Arman,

Oleg Larionov,

Michael P. Doyle

Department of Chemistry, The University of Texas at San Antonio, San Antonio, Texas 78249, United States

### Abstract

One of the most important reactions of 1,2,3-triazines with a dienophile is inverse electron demand Diels–Alder (IEDDA) cycloaddition, which occurs through nucleophilic addition to the triazine followed by N<sub>2</sub> loss and cyclization to generate a heterocycle. The site of addition is either at the 4- or 6-position of the symmetrically substituted triazine core. Although specific examples of the addition of nucleophiles to triazines are known, a comprehensive understanding has not been reported, and the preferred site for nucleophilic addition is unknown and unexplored. With access to unsymmetrical 1,2,3-triazine-1-oxides and their deoxygenated 1,2,3-triazine compounds, we report C-, N-, H-, O-, and S-nucleophilic additions on 1,2,3-triazine and 1,2,3-triazine-1-oxide frameworks where the 4- and 6-positions could be differentiated. In the IEDDA cycloadditions using C- and N-nucleophiles, the site of addition is at C-6 for both heterocyclic systems, but product formation with 1,2,3-triazine-1-oxides is faster. Other N-nucleophile reactions with triazine 1-oxides show addition at either the 4- or 6-position of the triazine 1-oxide ring, but nucleophilic attack only occurs at the 6-position on the triazine. Hydride from NaBH<sub>4</sub> undergoes addition at the 6-position on the triazine and the triazine 1-oxide core. Alkoxides show a high nucleophilic selectivity for the 4-position of the triazine 1-oxide. Thiophenoxide, cysteine, and

oleg.larionov@utsa.edu, michael.doyle@utsa.edu.

Author Contributions

L.D.A., G.C.H., and G.R. contributed equally.

Supporting Information

The Supporting Information is available free of charge at <https://pubs.acs.org/doi/10.1021/jacs.3c01347>.

● Experimental procedure; DFT calculations and spectroscopic data for all new compounds; and X-ray crystallographic data for **2**, **3**, **6**, **8a**, and **14a**

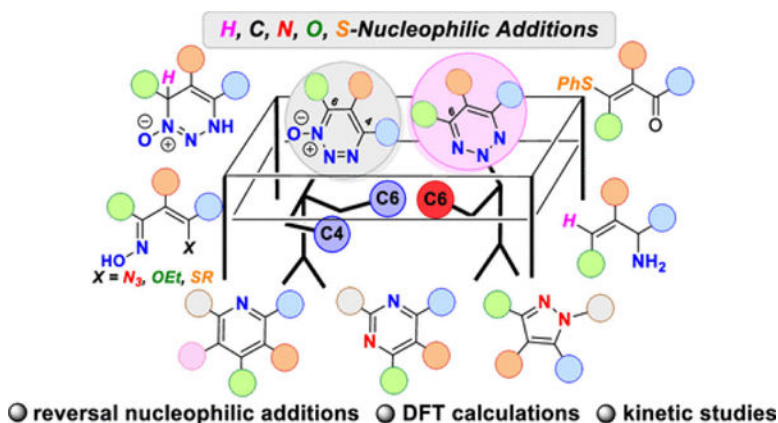
Accession Codes

CCDC 2088139, 2125940, 2125942, 2163136, 2205896, 2206098, and 2250486 contain the supplementary crystallographic data for this paper. These data can be obtained free of charge via [www.ccdc.cam.ac.uk/data\\_request/cif](http://www.ccdc.cam.ac.uk/data_request/cif), or by emailing [data\\_request@ccdc.cam.ac.uk](mailto:data_request@ccdc.cam.ac.uk), or by contacting The Cambridge Crystallographic Data Centre, 12 Union Road, Cambridge CB2 1EZ, UK; fax: +44 1223 336033.

The authors declare no competing financial interest.

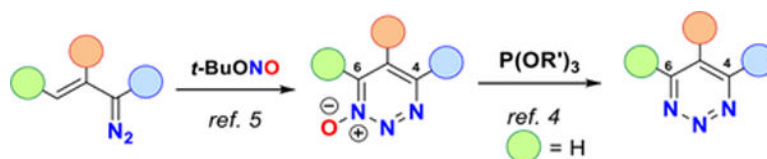
glutathione undergo nucleophilic addition on the triazine core at the 6-position, while addition occurs at the 4-position of the triazine 1-oxide. These nucleophilic additions proceed under mild reaction conditions and show high functional group tolerance. Computational studies clarified the roles of the nucleophilic addition and nitrogen extrusion steps and the influence of steric and electronic factors in determining the outcomes of the reactions with different nucleophiles.

## Graphical Abstract



## Introduction

1,2,3-Triazines represent an important class of heterocycles that has proven to be a valuable synthetic scaffold due to their efficient uses in the synthesis of a variety of N-heterocycles<sup>1</sup> and important pharmaceutical targets<sup>2</sup> because of their biological activities and therapeutic applications. However, their chemistries, especially their reactions with nucleophiles, are virtually unknown. Recently, the inverse electron demand Diels–Alder (IEDDA) reaction between 1,2,3-triazines and amidines, previously thought to occur by Diels–Alder addition/retro-Diels–Alder expulsion of dinitrogen, has been acknowledged as possibly occurring by a nucleophilic addition/N<sub>2</sub> elimination/cyclization pathway (Scheme 1a).<sup>3</sup> The site of nucleophilic addition is at either the 4- or 6-position of the substitution-symmetrical 1,2,3-triazine core, but evidence presented thus far has not allowed distinction between these two centers because the triazines that have been examined have been substitution-symmetrical. Our recent access to 1,2,3-triazine-4-carboxylates 1-oxides<sup>4</sup> and, following deoxygenation, their parent 1,2,3-triazine-4-carboxylates<sup>5</sup> (eq 1) provides substrates through which the 4- and 6-positions could be differentiated.



(Eq1)

Investigating reactions of 1,2,3-triazine 1-oxides with a variety of nucleophiles (Scheme 1b), we uncovered a divergence in reactivity with carbon and nitrogen nucleophiles, and by borohydride undergoing addition to the 6-position, while azides, alkoxides, and thiols reacted at the 4-position. To our surprise, these nucleophiles (H, C, N, and S) underwent nucleophilic attack on 1,2,3-triazines only at the 4-position (Scheme 1c). We report herein systematic experimental and computational investigations that unraveled remarkable structural effects underlying the divergence in reactivity of diverse nucleophiles with 1,2,3-triazine 1-oxides and 1,2,3-triazines.

## Results and Discussion

Classic IEDDA conversions of 1,2,3-triazines with  $\beta$ -ketoesters to form pyridines<sup>6</sup> and with amidines to form 1,3-diazines<sup>7</sup> occur in high yields under mild conditions. Treatment of ethyl 5-phenyl-1,2,3-triazine-4-carboxylate **1a** in the presence of a base and methyl 3-oxopentanoate formed ethyl 2-ethyl-5-methylcarboxylato-3-phenylpyridine-2-carboxylate **2** and with benzamidine formed ethyl 2,5-diphenylpyrimidine-4-carboxylate **3**,<sup>8</sup> whose structures were confirmed by X-ray crystallography, in high yields under mild conditions (Scheme 2). The site of nucleophilic attack in both cases is the 6-position of the 1,2,3-triazine ring. Since **1** was formed from its 1-oxide, ethyl 5-phenyl-1,2,3-triazine-4-carboxylate 1-oxide **4a**, we also performed the same reactions on identically substituted 1,2,3-triazine 1-oxide **4a** with methyl 3-oxopentanoate and benzamidine, which formed the same pyridine (**2**) and pyrimidine (**3**) products as from triazine **1a** in near quantitative yields under the same mild conditions. Furthermore, efforts to optimize the yield of **2** and **3** revealed that 1,1,1,3,3,3-hexafluoro-2-propanol (HFIP), known for its activation of cycloadditions,<sup>3b,9</sup> did not accelerate these IEDD cycloadditions (Supporting Information, Tables S1 and S2). To substantiate the evolution of N<sub>2</sub>O in the IEDDA cycloadditions with **4**, IR analysis of the atmosphere above the reaction solution was determined, and strong absorbance peaks at 2213.1 and 2235.7 cm<sup>-1</sup> were observed, as well as were their overtones at 2550 and 3460 cm<sup>-1</sup>, which are characteristic of N<sub>2</sub>O.<sup>10</sup> Notably, the two transformations differ only in their gaseous extrusion: N<sub>2</sub> from **1a** or N<sub>2</sub>O from **4a**.

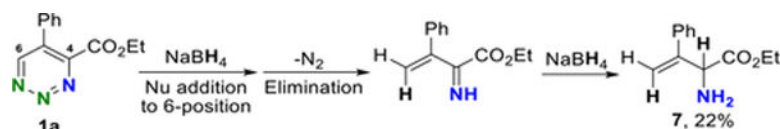
To determine the rate of each reaction, the time courses for reactions between methyl 3-oxopentanoate with triazine **1a** and triazine 1-oxide **4a** were monitored by <sup>1</sup>H NMR (0.1 M, CDCl<sub>3</sub>) (Figures S1 and S2). Triazine **1** is consumed very slowly, and after 65 min, its molar amount is still more than 40% with product **2** formation barely at 60% (Figure S1). In contrast, the consumption of triazine 1-oxide **4a** occurs very rapidly, and just after 12 min, its molar amount is 20%, while the amount of pyridine **2** is 80% (Figure S2). The data acquired fit second-order kinetics from which the rate constants,  $k_{\text{triazine 1-oxide}}$  and  $k_{\text{triazine}}$ , were calculated to be 2.39 and  $0.217 \times 10^{-2} \text{ M}^{-1} \text{ s}^{-1}$ , respectively. Thus, the rate of product formation from triazine 1-oxide **4a** is 10-fold faster than that from triazine **1a** when the same reactions are performed under the exact same conditions (Figure 1A). Intrigued by this substantial difference in rate for product formation with the  $\beta$ -ketoester, the progress of the reaction between benzamidine and triazine **1a** and triazine 1-oxide **4a** was also monitored by <sup>1</sup>H NMR spectroscopy (Figures S3 and S4). In less than 30 min, the molar amount of 1,2,3-triazine 1-oxide **4a** is 20% and the amount of the diazine product **3** is 80% (Figure S3).

Similarly, diazine **3** is obtained in 80% yield after 35 min from 1,2,3 triazine **1a** under the same reaction conditions (Figure S4). From the NMR studies, the second-order constants of this IEDDA cycloaddition between benzamidine and 1,2,3-triazine 1-oxide and 1,2,3 triazine were determined to be  $k_{\text{triazine 1-oxide}} = 1.04 \times 10^{-2} \text{ M}^{-1} \text{ s}^{-1}$  and  $k_{\text{triazine}} = 0.809 \times 10^{-2} \text{ M}^{-1} \text{ s}^{-1}$  demonstrating that product formation from triazine 1-oxide **4** is 1.4-fold faster than that from triazine **1** when the same reactions are performed under the exact same conditions (Figure 1B).

To further determine if the same site selectivity occurs in reactions with other N-nucleophiles, we studied the reaction of **1a** and **4a** with MeNHNH<sub>2</sub> and TMSN<sub>3</sub>. Treatment of **4a** with MeNHNH<sub>2</sub> in a DCE solution at room temperature generated after 3 h the corresponding pyrazole compound **5** in high yield (Scheme 3a). The reaction proceeded by nucleophilic addition at C-6 followed by N<sub>2</sub>O extrusion and intramolecular cyclization with elimination of NH<sub>3</sub>. Under the same reaction conditions, triazine **1a** produced the same pyrazole **5** in 65% yield. Surprisingly, when TMSN<sub>3</sub> and triazine 1-oxide **4a** were used in a MeOH solution at 45 °C for 12 h, site selectivity was reversed, and addition occurred at the 4-position to furnish in modest yield the corresponding enoxime **6**, whose structure was confirmed by X-ray crystallography (Scheme 3b). In contrast to what was observed from the reactions with MeNHNH<sub>2</sub> and benzamidine, the addition of azide from TMSN<sub>3</sub> is selective at C-4, which is followed by N<sub>2</sub> elimination and protonation to obtain the enoxime **6**. Instead, the treatment of TMSN<sub>3</sub> with triazine **1a** produced multiple intractable materials from which no major product was identified, and **6** was not detected.

To determine if the same site selectivity occurs in reactions with other nucleophiles, we have examined reactions of **1** and **4** with borohydride, ethoxide, and thiols, which have received scant or no prior attention. Sodium borohydride (NaBH<sub>4</sub>) is a common tool in organic chemistry for mild reductions of heterocycles;<sup>11</sup> yet, electron rich heterocycles such as pyridines react with NaBH<sub>4</sub> under harsh conditions only if they carry electron withdrawing substituents, especially in the 3-position.<sup>12</sup> In contrast, the corresponding pyridine *N*-oxide, whose ring is electron-deficient, reacts with NaBH<sub>4</sub> in refluxing ethanol to effect reduction and deoxygenation.<sup>13</sup> The *N*-oxide on pyridine derivatives activates the 2- and 4-positions of these heterocycles for nucleophilic addition.<sup>14</sup> Borohydride addition to 4-methyl-6-phenyl-1,2,3-triazine is reported to occur at position 5 to form the 2,5-dihydro triazine.<sup>15</sup> However, Ohsawa and co-workers showed that the reduction of 1,2,3-triazine 2-oxide is not selective, based on deuterium labeling experiments, and occurs at positions 4 and 6 to furnish the fully reduced tetrahydro-1,2,3-triazine-2-oxide in which the *N*-oxide group remained intact.<sup>16</sup> The same group subsequently reported a different outcome when a 1,2,3-triazine 1-oxide reacted with NaBH<sub>4</sub>.<sup>15,16</sup> Based only on <sup>1</sup>H NMR spectra, the authors proposed that the reduction reaction is selective at position 5 and proceeded with spontaneous deoxygenation to deliver 2,5-dihydro-1,2,3-triazine as the only product.

Treatment of **1a** with sodium borohydride in MeOH at 0 °C for 4 h produced the corresponding the  $\alpha$ -amino acid ester **7**, albeit in very low yield. This product is consistent with nucleophilic addition occurring at position 6 and followed by N<sub>2</sub> elimination, then by imine reduction (eq 2).<sup>17</sup> Nucleophilic attack at position 6 on triazine **1a** is in agreement with Boger's mechanistic proposal of stepwise nucleophilic addition.<sup>3a</sup>



(Eq. 2)

Surprisingly, the reduction of triazine 1-oxide **4a** with NaBH<sub>4</sub> in MeOH at 0 °C was complete within 30 min but did not undergo deoxygenation to produce the corresponding 2,5-dihydro-1,2,3-triazine, as was reported by Ohsawa.<sup>15,16</sup> Instead, 3,6-dihydro-1,2,3-triazine 1-oxide **8a**, whose structure was confirmed by X-ray crystallography, was produced in 70% yield (Table S3). Milder or stronger reducing agents, sodium triacetoxyborohydride or lithium aluminum hydride,<sup>18</sup> furnished dihydrotriazine 1-oxide **8a** in only trace amounts. 2,2,2-Trifluoroethanol (TFE) and 1,1,1,3,3,3-hexafluoro-2-propanol (HFIP) increased the solubility of the triazine 1-oxide **4a** and the yield and therefore were more suitable solvents for the reduction of triazine oxide **4a** with NaBH<sub>4</sub>. Under optimized conditions 2,5-dihydrotriazine 1-oxide **8a** was formed in 94% isolated yield in just 4 h by slow addition of **4a** into a vial containing only 50 mol % of NaBH<sub>4</sub> in 2,2,2-trifluoroethanol at 0 °C.

With the optimized conditions in hand, the generality of the synthesis of 3,6-dihydro-1,2,3-triazine-4-carboxylate 1-oxides **8** through reduction of **4** with NaBH<sub>4</sub> was examined (Scheme 4). An array of 5-aryl-1,2,3-triazine 1-oxides bearing either electron donating groups (EDG) (**4a-4e**) or electron withdrawing groups (EWG) (**4f-4g**) furnished the corresponding 2,5-dihydrotriazine 1-oxides in excellent yield. The mild reduction conditions allowed high functional group compatibility and tolerance to a variety of functional groups. Substituted triazine 1-oxides bearing functional groups such as azide, phenylalkyl, *tert*-butyldimethylsilyl ether (OTBS), and alkyl were converted into the corresponding dihydrotriazine 1-oxides **8h-8k** in high yields, as was the 5,6-unsubstituted triazine-4-carboxylate **8l**. To further demonstrate the generality of this method, more constrained five- and six-membered bicyclic triazine-4-carboxylate 1-oxides (**4m** and **4n**) formed the desired products in good to high yields. Potential late-stage functionalization by this method was examined using **4o**, which was directly derivatized from the steroid hormone epiandrosterone, which was converted to the dihydrotriazine 1-oxide **5o** in 65% isolated yield. Mechanistically, similar to what was observed with **1a**, the hydride from NaBH<sub>4</sub> selectively undergoes nucleophilic addition at the electrophilic 6-position of the triazine oxide **4**. However, instead of undergoing the loss of nitrous oxide (dinitrogen in the case of **1**), the anionic intermediate is protonated by the solvent to form 3,6-dihydro-1,2,3-triazine-4-carboxylate 1-oxides **8**.

To explain this selective borohydride addition at position 6 of the triazine 1-oxide **4**, density functional theory (DFT) calculations were performed to investigate the mechanism and to gain insights into the observed nucleophile-dependent divergent reactivity. The hydride addition from borohydride at the C6 position of the triazine 1-oxide ring proceeded via a substantially lower barrier ( $G^\ddagger = 17.9$  kcal/mol for **TS2-C6**) than hydride addition at the C4 position ( $G^\ddagger = 23.8$  kcal/mol for **TS1-C4**) (Figure 2A), which is in line with

the experimental observations. Interestingly, while nitrogen extrusion from the resulting energetically preferred C6-reduction intermediate **9** was found to be precluded by the prohibitively high activation barrier ( $G^\ddagger = 40.0$  kcal/mol for **TS4-C6**) en route to strained azetidine **10**, dinitrogen extrusion in the C4-selective pathway was, by comparison, kinetically accessible ( $G^\ddagger = 8.8$  kcal/mol for **TS3-C4**). However, the high C6 selectivity of the reduction step ( $G^\ddagger = 6.4$  kcal/mol) precluded accumulation of C4-intermediate **11** that would be required to access the irreversible dinitrogen extrusion step en route to acyclic product **12**, resulting in the formation of the experimentally observed dihydrotriazine 1-oxide **8a**. Taken together, these results account for the observed C6 selectivity of the borohydride-mediated reduction and are in agreement with the experimental isolation of the product derived from N-protonation of **9**.

Activation-strain distortion/interaction analysis<sup>19</sup> was performed to examine the factors influencing the observed C6-selective reduction (Figure 2B). This analysis indicated that reduction at C4, proceeding through **TS1-C4**, is associated with a substantially higher distortion energy (16.7 kcal/mol, cf., 11.0 for **TS2-C6**) and only slightly higher stabilizing interactions ( $-7.4$  kcal/mol cf.,  $-6.3$  kcal/mol for **TS2-C6**). Decomposition of the distortion energies associated with achieving either transition state structure on a per-fragment basis revealed a smaller difference in distortion for the borohydride fragment. By contrast, the triazine *N*-oxide ring fragment suffers from a more significant distortion en route to **TS1-C4**, suggesting that the smaller distortion of the triazine ring on the pathway traversing **TS2-C6** is responsible for the observed C6-selectivity (Figure 2B,C), as expected for a reaction occurring at a less sterically congested C6 site and at the relatively short distances between the incoming nucleophile and the reacting triazine 1-oxide carbon in both **TS1-C4** and **TS4-C6** (1.40 and 1.46 Å). The increased steric encumbrance for the addition to C4 is also evident from an energy decomposition analysis (EDA)<sup>20</sup> of the two regioselectivity-determining transition state structures **TS1-C4** and **TS2-C6** that revealed a substantially greater destabilizing Pauli repulsion in **TS1-C4** than in **TS2-C6** (Figure 2D). The greater Pauli repulsion in **TS1-C4** is compensated by stronger electrostatic and charge transfer interactions, with the donation from the borohydride HOMO to the triazine 1-oxide LUMO for **TS1-C4** and LUMO + 1 for **TS2-C6** as the dominant charge transfer contributions, as indicated by an analysis of complementary occupied-virtual pairs (COVPs)<sup>21</sup> (Figure 2E).

In our endeavor to determine if the selectivity observed with carbon, nitrogen, and hydride nucleophiles is general, we further evaluated nucleophilic addition reactions using stronger nucleophiles including alkoxide (RO<sup>-</sup>) and thiolates (ArS<sup>-</sup> and RS<sup>-</sup>). We speculated that ethoxide or thiolates could undergo addition to the more electrophilic C-4 position, being adjacent to the electron-withdrawing carboxylate group.

With 1,2,3-triazine 1-oxide **4** nucleophilic attack at position 4 was expected to form a conjugated oxime followed by loss of molecular nitrogen. Enoximes are important scaffolds in organic synthesis for the preparation of  $\alpha,\beta$ -unsaturated carbonyl compounds,<sup>22</sup> nitriles,<sup>23</sup> pyridines,<sup>24</sup> and pyrazole-*N*-oxides.<sup>25</sup> Moreover, enoximes have also demonstrated biological properties as contact allergens.<sup>26</sup> 1,2,3-Triazine 1-oxide **4a** and NaOEt were chosen to evaluate selective nucleophilic addition. Remarkably, in ethanol, triazine 1-oxide

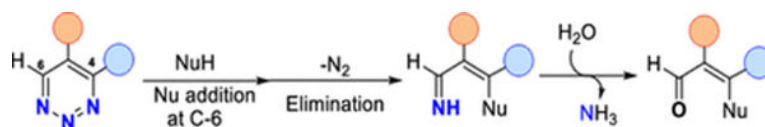
**1a** was converted into the conjugated enoxime **13a** as the only product (83% isolated yield) in less than 1 h. In addition to being selective for addition to the 4-position, this nucleophilic reaction is also diastereoselective, producing only one geometrical isomer.

After finding the optimum conditions using 1.2 equiv. of EtONa in ethanol at room temperature (Table S4), an array of enoximes was prepared from the selective O-nucleophilic addition at the 4-position of 1,2,3-triazine 1-oxides **4** (Scheme 5). Triazine 1-oxide bearing either EDG or EWG (**4b–c**, **4f**, and **4p**) were converted to the corresponding enoximes **13b–p** in high yields but, more importantly, a simple quench and extraction makes this reaction very practical by not necessitating the use of column chromatography. Conjugated enoximes with hydrogen as R<sub>1</sub> and R<sub>2</sub> as ethyl **13q** or borneol **13r** carboxylates were selectively prepared in moderate to good yields. 1,2,3-Triazine 1-oxides with an alkyl group in position 5 (isopropyl **4s**, cyclopropyl **4t**, and cyclopentyl **4u**) furnished the corresponding enoximes **13s–u** with excellent dr ratios. Notably, phenols, including tyrosine, did not undergo nucleophilic addition, and the reactants were recovered unchanged. However, thiophenolate, generated in situ from thiophenol and triethylamine in methylene chloride (Table S5), underwent nucleophilic addition at the same 4-position to furnish enoxime **14a** in 95% yield. In addition, sulfur containing amino acid derivatives l-cysteine methyl ester hydrochloride and l-glutathione dimethyl ester hydrochloride were compatible for this protocol and provided cysteine/glutathione-substituted enoxime **14b–c** in very good isolated yields (81–88%) at room temperature without evidence of any reaction with the amino functional group. This highly selective thiolate reaction has potential applications for protein modifications.<sup>27</sup>

The selective methoxide addition at position 4 of the triazine 1-oxide **1** was also corroborated computationally (Figure 3A) by a lower barrier to the methoxide addition ( $G^\ddagger = 1.5$  kcal/mol) in the C4 pathway ( $-5.9$  kcal/mol for **TS5-C4**, cf.,  $-4.4$  kcal/mol for **TS6-C6**). Interestingly, although greater distortion was observed for **TS5-C4** than for **TS6-C6** (Figure 3B), mirroring steric effects for attack at the more congested C4 site observed for borohydride reduction, methoxide addition to C4 proceeded with a substantially higher interaction energy, resulting in a smaller activation barrier. EDA of transition states **TS5-C4** and **TS6-C6** indicated that the higher interaction energy of **TS5-C4** is due to greater contributions of charge transfer, dispersion, and polarization (Figure 3C). The strong effect of charge transfer on the C4 selectivity was confirmed by analysis of COVPs that revealed a significantly stronger dominant HOMO  $\rightarrow$  LUMO + 1 charge transfer in **TS5-C4** than in **TS6-C6** (Figure 3D). The reduced steric repulsion and increased interactions for the reaction with methoxide are in line with the longer distance between the nucleophile and the reacting site (1.92 and 2.55 Å for **TS5-C4** and **TS6-C6**) and the higher HOMO energy ( $-5.66$  eV for methoxide and  $-7.88$  eV for borohydride), resulting in the reversal of selectivity in favor of C4 addition. Dinitrogen extrusion is readily accessible for the reaction with methoxide from C4 addition intermediate **15** via **TS7-C4** ( $G^\ddagger = 13.6$  kcal/mol), resulting in the exergonic formation of E-product **16**, consistent with the experimental observations. Furthermore, in parallel to the reactivity observed in the borohydride reduction, the barrier to dinitrogen extrusion from intermediate **17** in route to azetidine **18** in the C6 pathway was prohibitively high, restricting the methoxide system to the kinetically facile C4 pathway. A

broadly similar kinetic profile was observed for the reaction with thiophenolate (Figure S10 in the Supporting Information), i.e., selectivity was determined by the lower-barrier nitrogen extrusion in the C4 pathway despite the kinetic preference for the C6 position in the addition step.

With 1,2,3-triazines **1**, nucleophilic attack at position 4 was expected to form aldehyde derivatives after loss of N<sub>2</sub> and subsequent imine hydrolysis (eq 3).<sup>28</sup> However, a different outcome occurred when PhSH was added to triazine **1** in the presence of a base as triethylamine. Thiophenoxide underwent nucleophilic addition at the 6-position to furnish in high yield the sulfide compound **19** after N<sub>2</sub> elimination and hydrolysis of imine (eq 4).



(Eq. 3)



(Eq. 4)

The presence of imine intermediate **A** was observed by HRMS, and the configuration of **19** was established by NOE correlation between the vinyl hydrogen and the aromatic protons on both phenyl rings. In contrast, treatment of EtO<sup>-</sup> with triazine **1a** produced a complex mixture of byproducts from which no major product was identified, and products anticipated from attack at either the 4- or 6-position (eq 3 and eq 4) were not detected.

## Conclusions

In conclusion, 1,2,3-triazine 1-oxides showed similarities, but remarkable differences, with 1,2,3-triazines in nucleophilic addition reactions. In particular, the site of addition in 1,2,3-triazines 1-oxide was the same as that for 1,2,3-triazine in IEDD cycloadditions, and C or N addition occurred at the 6-position followed by N<sub>2</sub>O/N<sub>2</sub> elimination and cyclization pathways, but triazine 1-oxide exhibited an enhanced rate of product formation. The site of addition in the triazine 1-oxide core was reversed when TMSN<sub>3</sub> was applied, which occurred at the 4-position to form enoximes. Hydride addition from NaBH<sub>4</sub> occurred at the 6-position of both N-heterocycles but furnished different products and yield, the probable cause for which is explained. Sulfide addition to 1,2,3-triazine also occurred at position 6. However, the addition of O and S nucleophiles to triazine 1-oxides showed a reversal in the site of addition, preferring the 4-position to obtain enoximes. Our computational studies, which include activation-strain distortion/interaction analysis, have provided a detailed



description of the structural and electronic effects that are responsible for the divergent outcomes observed in the reactions of triazine 1-oxides with different nucleophiles. While the less substituted C6 position favors the attack by a nucleophile that is sensitive to steric encumbrance (i.e., borohydride, due to the shorter forming C–H bond), the reaction with methoxide benefits from stronger interactions at the C4 position. Finally, the kinetic facility of nitrogen extrusion after the C4 addition of methoxide and thiophenolate leads to the formation of enoximes.

## Supplementary Material

Refer to Web version on PubMed Central for supplementary material.

## Acknowledgments

Support for this research from the Welch Foundation (AX-1871 to M.P.D. and AX-0047 to O.L.) and NIGMS (GM13437 to O.L.) is gratefully acknowledged. The X-ray diffractometer used in this research was supported by a grant from the U.S. National Science Foundation (CHE-1920057).

## References

- 1). (a) Zhang J; Shukla V; Boger DL Inverse Electron Demand Diels-Alder Reaction of Heterocyclic Azadienes, 1-Aza-1,3-Butadienes, Cyclopropanone Ketals and Related Systems. A Retrospective. *J. Org. Chem* 2019, 84, 9397–94455. [PubMed: 31062977] (b) Zhang F-G; Chen Z; Tang X; Ma J-A Triazines: Syntheses and Inverse Electron-demand Diels–Alder Reactions. *Chem. Rev* 2021, 121, 14555–14593. [PubMed: 34586777]
- 2). (a) Mfuh AM; Larionov O; Larionov OV Heterocyclic N-Oxides - An Emerging Class of Therapeutic Agents. *Curr. Med. Chem* 2015, 22, 2819–2857. [PubMed: 26087764] (b) Larionov OV Heterocyclic N-Oxides; Springer International Publishing: Cham, Switzerland, 2018.(c) Cascioferro S; Parrino B; Spano V; Carbone A; Montalbano A; Barraja P; Diana P; Cirrincione G Synthesis and antitumor activities of 1,2,3-triazines and their benzo- and heterofused derivatives. *Eur. J. Med. Chem* 2017, 142, 74–86. [PubMed: 28615111]
- 3). (a) Wu ZC; Houk KN; Boger DL; Svatunek D Mechanistic Insights into the Reaction of Amidines with 1,2,3-Triazines and 1,2,3,5-Tetrazines. *J. Am. Chem. Soc* 2022, 144, 10921–10928. [PubMed: 35666564] (b) Yang Y-F; Yu P; Houk KN Computational Exploration of Concerted and Zwitterionic Mechanisms of Diels–Alder Reactions between 1,2,3-Triazines and Enamines and Acceleration by Hydrogen-Bonding Solvents. *J. Am. Chem. Soc* 2017, 139, 18213–18221. [PubMed: 29161031]
- 4). De Angelis L; Zheng H; Perz MT; Arman H; Doyle MP Intermolecular [5+1]-Cycloaddition between Vinyl Diazo Compounds and tert-Butyl Nitrite to 1,2,3-triazine 1-Oxide and Their Further Transformation to Isoxazole. *Org. Lett* 2021, 23, 6542–6546. [PubMed: 34370472]
- 5). Biswas S; De Angelis L; Rivera G; Arman H; Doyle MP; Doyle MP Inverse Electron Demand Diels–Alder-Type Heterocycle Syntheses with 1,2,3-Triazine 1-Oxides: Expanded Versatility. *Org. Lett* 2023, 25, 1104–1108. [PubMed: 36787541]
- 6). Zhang Y; Luo H; Lu Q; An Q; Li Y; Li S; Tang Z; Li B Access to Pyridines via Cascade Nucleophilic Addition Reaction of 1,2,3-Triazines with Activated Ketones or Acetonitriles. *Chin. Chem. Lett* 2021, 32, 393–396.
- 7). (a) Anderson ED; Boger DL Scope of the Inverse Electron Demand Diels-Alder Reactions of 1,2,3-Triazine. *Org. Lett* 2011, 13, 2492–2494. [PubMed: 21488676] (b) Anderson ED; Boger DL Inverse Electron Demand Diels–Alder Reactions of 1,2,3-Triazines: Pronounced Substituent Effects on Reactivity and Cycloaddition Scope. *J. Am. Chem. Soc* 2011, 133, 12285–12292. [PubMed: 21736324] (c) Anderson ED; Duerfeldt AS; Zhu K; Glinkerman CM; Boger DL Cycloadditions of Noncomplementary Substituted 1,2,3-Triazines. *Org. Lett* 2014, 16, 5084–8087. [PubMed: 25222918] (d) Glinkerman CM; Boger DL Synthesis,

- 8). Characterization, and Rapid Cycloadditions of 5-Nitro-1,2,3-triazine. *Org. Lett* 2018, 20, 2628–2631. [PubMed: 29659291]
- 9). A structure similar to compound 3 has been reported previously Huschka M; Gompper R; Polborn K CSD Communication (Private Communication), 2005, CCDC 292007.
- 10). Glinkerman CM; Boger DL Catalysis of Heterocyclic Azadiene Cycloaddition Reactions by Solvent Hydrogen Bonding: Concise Total Synthesis of Methoxatin. *J. Am. Chem. Soc* 2016, 138, 12408–12413. [PubMed: 27571404]
- 11). Nitrous Oxide; NISTWeb National Institute of Standards and Technology <https://webbook.nist.gov/cgi/cbook.cgi?ID=C10024972&Type=IR-SPEC&Index=1> (accessed Oct 03, 2022). (CAS RN: 10024-97-2).
- 12). Keay JG The Reduction of Nitrogen Heterocycles with Complex Metal Hydrides. *Adv. Heterocycl. Chem* 1986, 39, 1–77.
- 13). Yamada S; Kuramoto M; Kikugawa Y The Reaction of Cyanopyridines with Sodium Borohydride in Aprotic Solvents. *Tetrahedron Lett* 1969, 10, 3101–3104.
- 14). Jankovsky M; Ferles M Studies in the pyridine series. XXXVI. Some reductions of pyridine oxides and alkoxy pyridinium salts. *Collect. Czech. Chem. Commun* 1970, 35, 2802–2809.
- 15). (a) Londregan AT; Jennings S; Wei L Mild Addition of Nucleophiles to Pyridine N-Oxide. *Org. Lett* 2011, 13, 1840–1843. [PubMed: 21375291] (b) Fier PS A Bifunctional Reagent Designed for the Mild, Nucleophilic Functionalization of Pyridines. *J. Am. Chem. Soc* 2017, 139, 9499–9502. [PubMed: 28677963]
- 16). Ohsawa A; Arai H; Ohnishi H; Igeta H Synthesis, oxidation, and reduction of monocyclic 1,2,3-triazines. *J. Chem. Soc., Chem. Commun* 1980, 1182–1183.
- 17). Arai H; Ohsawa A; Ohnishi H; Igeta H Sodium Borohydride Reduction of Monocyclic 1,2,3-Triazine N-Oxide. *Heterocycles* 1982, 17, 317–320.
- 18). Billman JH; Diesing AC Reduction of Schiff Bases with Sodium Borohydride. *J. Org. Chem* 1957, 22, 1068–1070.
- 19). Heiden ZM; Lathem AP Establishing the Hydride Donor Abilities of Main Group Hydrides. *Organometallics* 2015, 34, 1818–1827.
- 20). Bickelhaupt FM; Houk KN Analyzing Reaction Rates with the Distortion/Interaction-Activation Strain Model. *Angew. Chem., Int. Ed* 2017, 56, 10070–10086.
- 21). (a) Horn PR; Sundstrom EJ; Baker TA; Head-Gordon M Unrestricted Absolutely Localized Molecular Orbitals for Energy Decomposition Analysis: Theory and Applications to Intermolecular Interactions Involving Radicals. *J. Chem. Phys* 2013, 138, 134119. [PubMed: 23574220] (b) Horn PR; Mao Y; Head-Gordon M Probing Non-Covalent Interactions with a Second-Generation Energy Decomposition Analysis using Absolutely Localized Molecular Orbitals. *Phys. Chem. Chem. Phys* 2016, 18, 23067–23079. [PubMed: 27492057]
- 22). Khaliullin RZ; Bell AT; Head-Gordon M Analysis of charge transfer effects in molecular complexes based on absolutely localized molecular orbitals. *J. Chem. Phys* 2008, 128, 184112. [PubMed: 18532804]
- 23). Shinada T; Yoshihara K A Facile Method for the Conversion of Oximes to Ketones and Aldehydes by the Use of Activated MnO<sub>2</sub>. *Tetrahedron Lett* 1995, 36, 6701–6704.
- 24). Brubaker AN; DeRuiter J; Whitmer WL Synthesis and rat lens aldose reductase inhibitory activity of some benzopyran-2-ones. *J. Med. Chem* 1986, 29, 1094–1099. [PubMed: 3086557]
- 25). Kellogg RM; Van Bergen TJ Reactions of aryl Grignard reagents with pyridine 1-oxide. Structure of the addition products. *J. Org. Chem* 1971, 36, 1705–1708.
- 26). Alcazar J; Almena I; Begtrup M; de la Hoz A Synthesis of 4hydroxylamino-1-azabuta-1,3-dienes and their cyclization to 2substituted pyrazole 1-oxides. *J. Chem. Soc., Perkin Trans 1* 1995, 2773–2781.
- 27). Nilsson A-M; Bergstrom MA; Luthman K; Nilsson JLG; Karlberg A-T An  $\alpha,\beta$ -unsaturated oxime identified as a strong contact allergen. *Food Chem. Toxicol* 2005, 43, 1627–1636. [PubMed: 15978713]
- 28). Chalker JM; Bernardes GJL; Lin YA; Davis BG Chemical Modification of Proteins at Cysteine: Opportunities in Chemistry and Biology. *Chem. Asian J* 2009, 4, 630–640. [PubMed: 19235822]

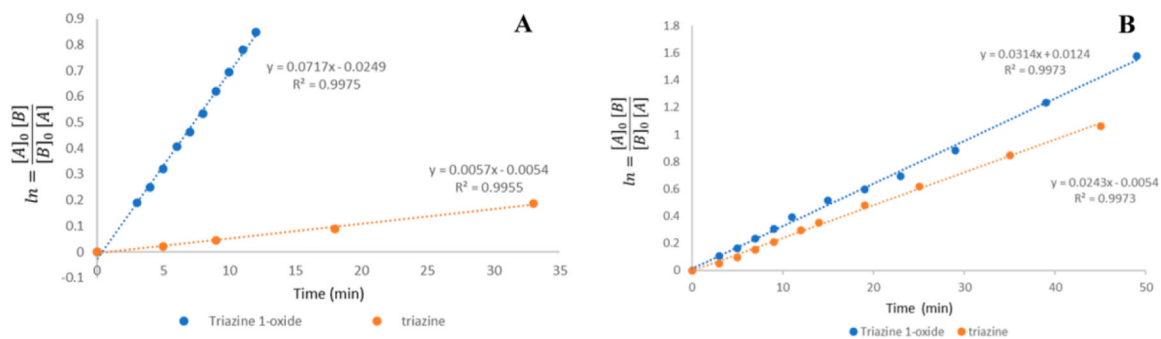
- 29). (a) Quiñones RE; Glinkerman CM; Zhu K; Boger DL Direct Synthesis of  $\beta$ -Aminoaldehydes through Reaction of 1,2,3-Triazine with Secondary Amines. *Org. Lett* 2017, 19, 3568–3571. [PubMed: 28657329] (b) Ohsawa A; Itoh T; Nagata K; Kaihoh T; Okada M; Kawabata C; Arai H; Ohnishi H; Yamaguchi K; Igeta H; Iitaka Y The Reactivity of Monocyclic 1,2,3-Triazine. *Heterocycles* 1992, 33, 631.

Author Manuscript

Author Manuscript

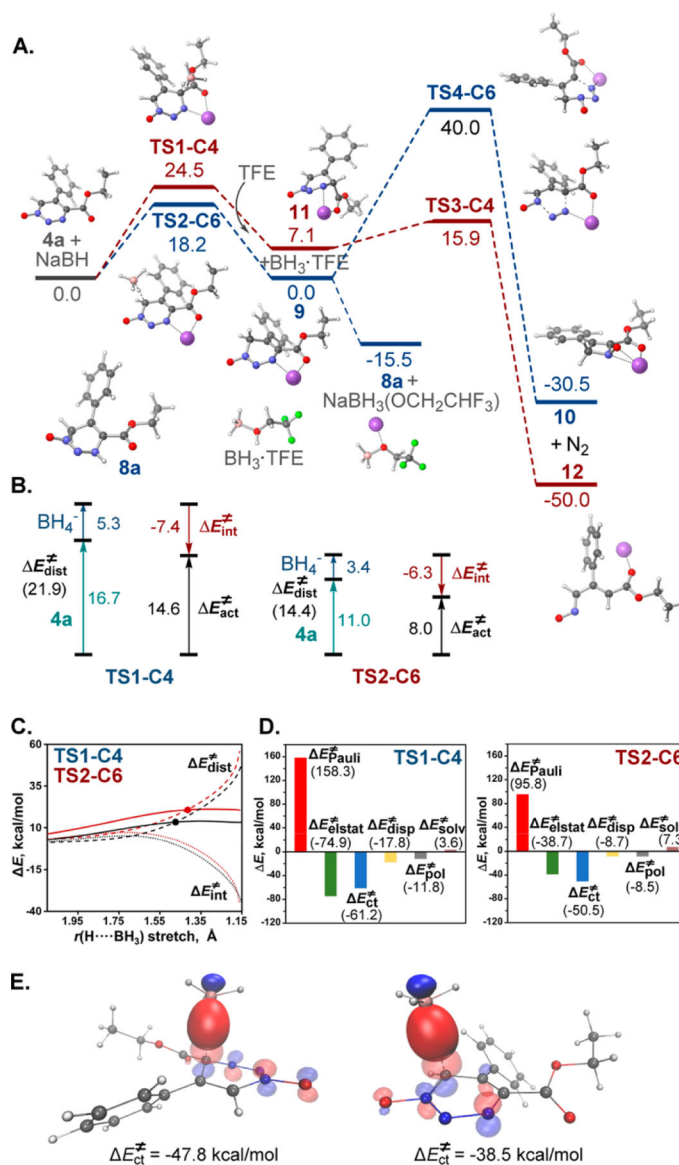
Author Manuscript

Author Manuscript



**Figure 1.**

(A) Linear fitting of triazine 1-oxide **4a** (blue) and triazine **1a** (orange) with methyl 3-oxopentanoate; (B) linear fitting of triazine 1-oxide (orange) and triazine (blue) with benzamidine.

**Figure 2.**

DFT computational studies of borohydride reduction of triazine 1-oxide **4a**. (A) Computed Gibbs free energy profile,  $G$ , kcal/mol. (B) Distortion/Interaction analysis for **TS1-C4** and **TS2-C6**. (C) Distortion/Interaction analysis for the C4 and C6 pathways. (D) Energy decomposition analysis for **TS1-C4** and **TS2-C6**. (E) Dominant complementary occupied-virtual pairs (COVPs) for **TS1-C4** and **TS2-C6**.

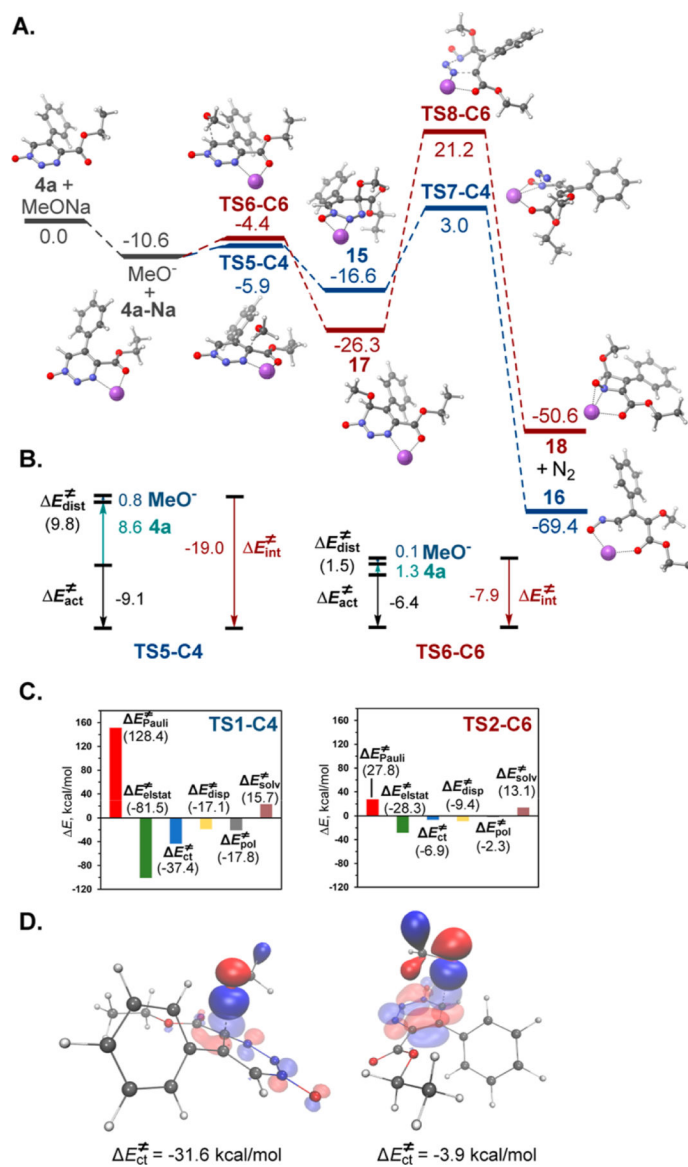
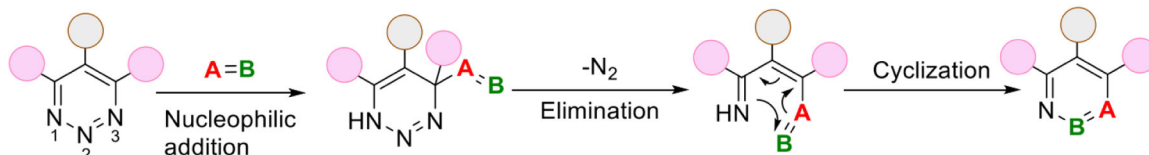
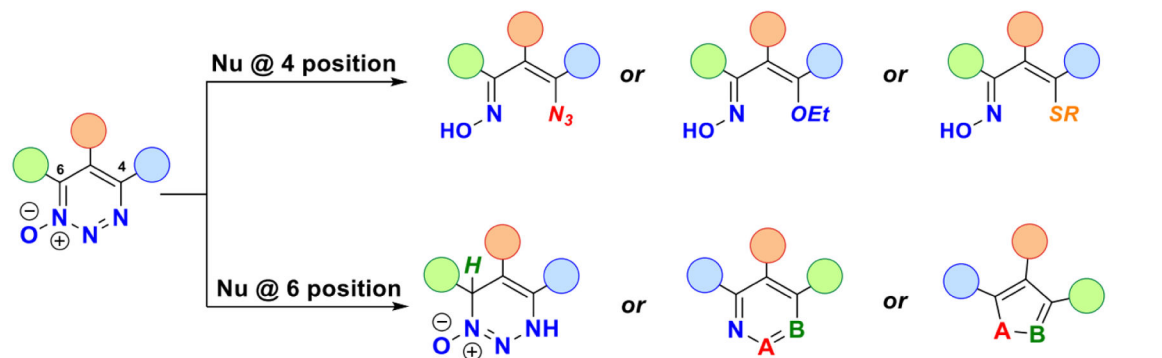


**Figure 3.** DFT computational studies of the methoxide reaction with triazine 1-oxide **S1**. (A) Computed Gibbs free energy profile,  $G$ , kcal/mol. (B) Distortion/interaction analysis for **TS5-C4** and **TS6-C6**. (C) EDA for **TS5-C4** and **TS6-C6**. (D) COVPs for **TS5-C4** and **TS6-C6**.

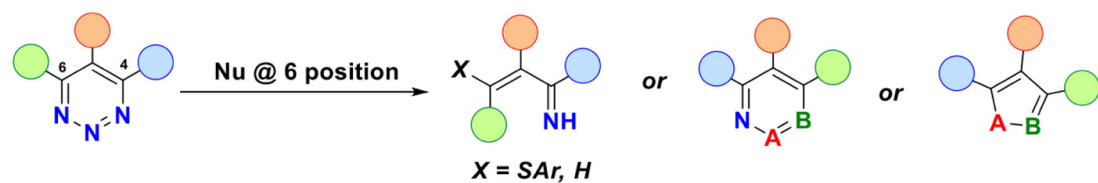
**a. Nucleophilic addition to 1,2,3-triazine (ref. 3)**



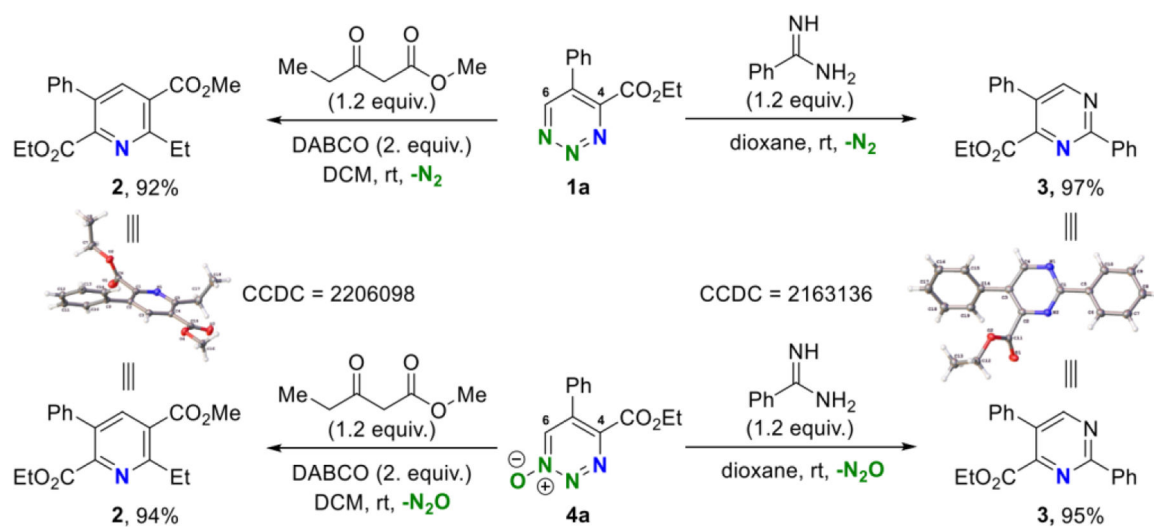
**b. H,C,N,S Nucleophilic addition to 1,2,3-triazine 1-oxide**



**c. H,C,N,S Nucleophilic addition to 1,2,3-triazine**



**Scheme 1.**  
Nucleophilic Addition to 1,2,3-Triazine and 1,2,3-Triazine 1-Oxide

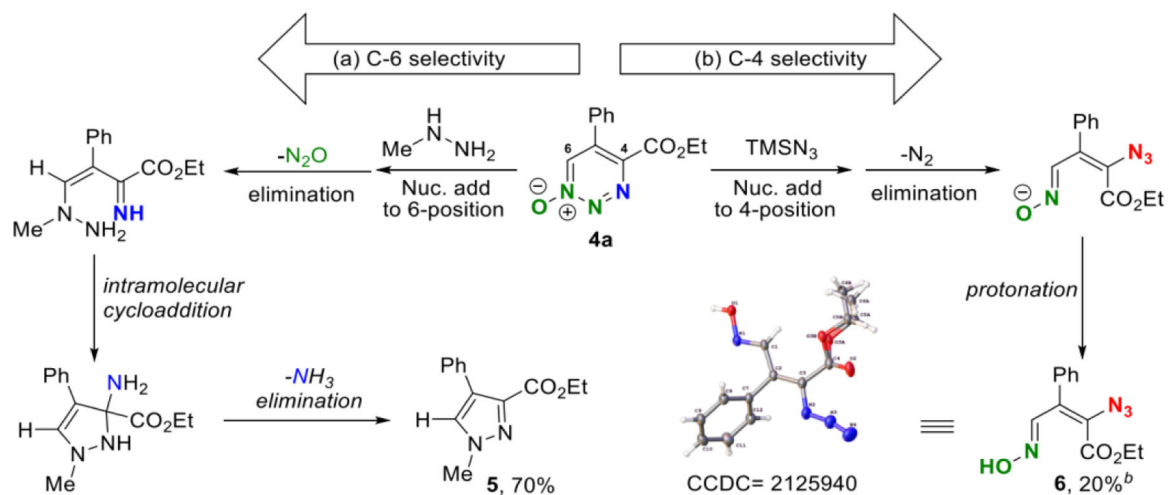
**Scheme 2.**

IEDD with 1,2,3-Triazine and 1,2,3-Triazine-1-oxide<sup>a</sup>

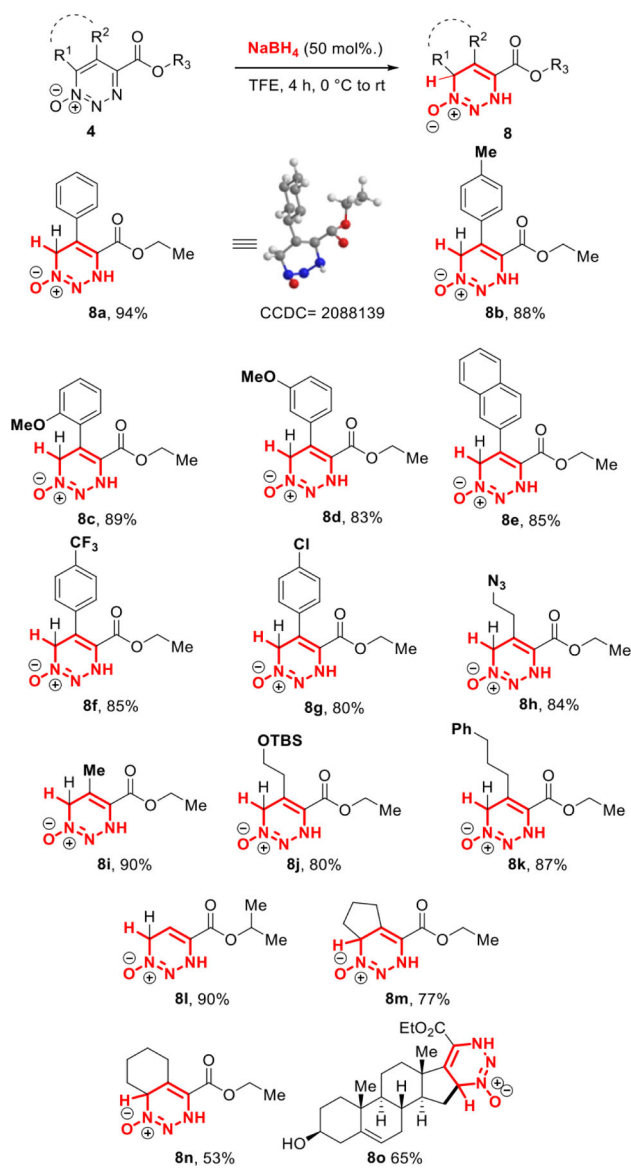
<sup>a</sup> Reaction conditions: **1** or **4** (0.1 mmol, 0.1 M in DCM) was added all at once to a vial containing methyl 3-oxopentanoate (1.2 equiv., 0.12 M) and DABCO (2.0 equiv.) at rt.

Benzamidine (1.2 equiv.) was added all at once to a vial containing **1** or **4** (0.1 mmol, 0.05 M in dioxane) at rt.

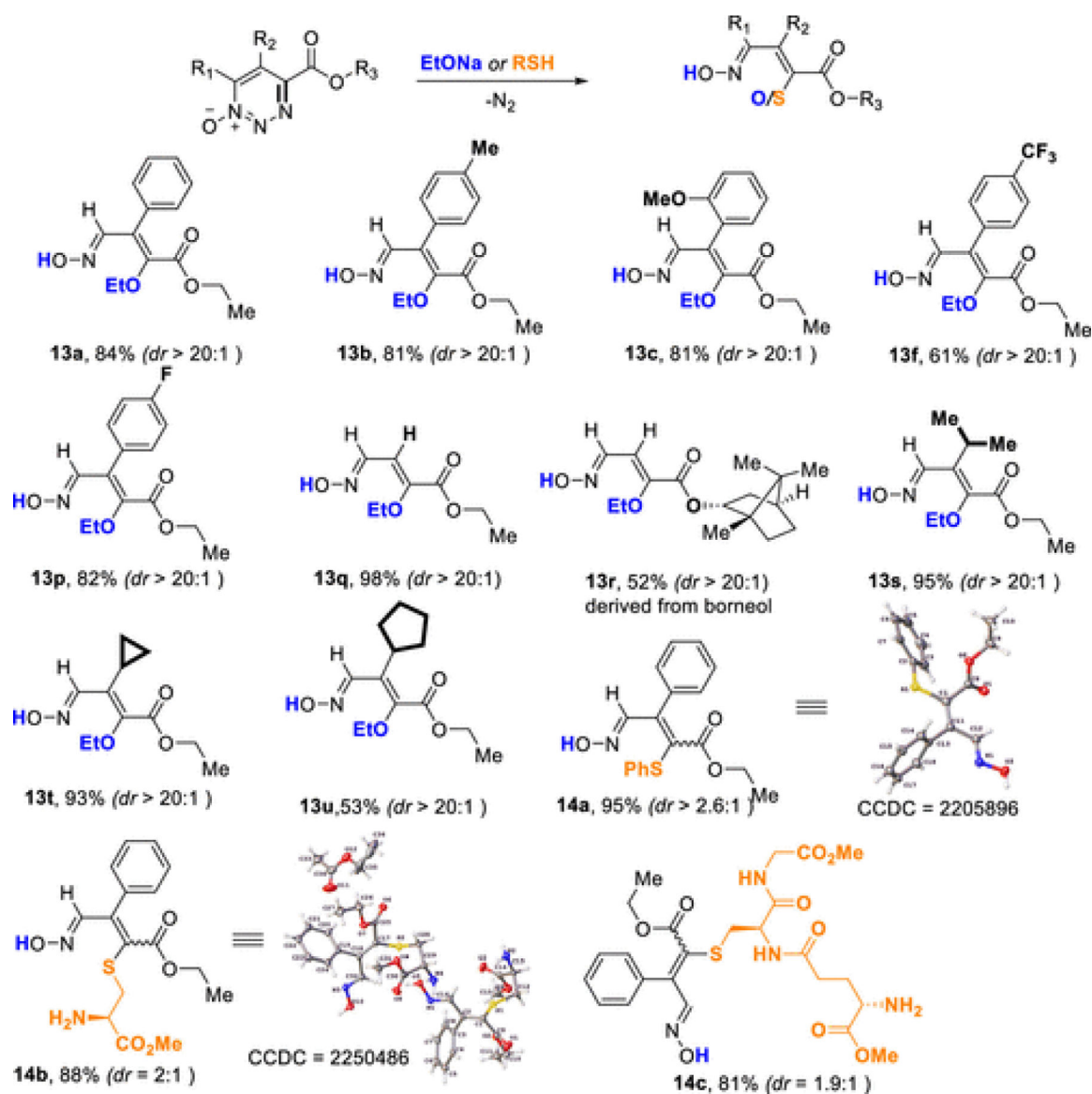


**Scheme 3.**Reverse Site of Nucleophilic Addition with N-Nucleophile <sup>a</sup>

<sup>a</sup> Reaction conditions. MeNHNH<sub>2</sub> as the nucleophile: MeNHNH<sub>2</sub> (1.5 equiv.) was added all at once in a vial containing **4a** (0.1 mmol, 0.05 M in DCE). The reaction was continued for 4 h at rt. TMSN<sub>3</sub> as the nucleophile: TMSN<sub>3</sub> (1.5 equiv.) was added all at once in a vial containing **4a** (0.1 mmol, 0.05 M in MeOH) at rt. The reaction was continued for 12 h at 45 °C. <sup>b</sup>71% of **4a** was recovered.

**Scheme 4.**Synthesis of 3,6-Dihydro Triazine-1-oxide with  $\text{NaBH}_4$ <sup>a</sup>

<sup>a</sup> Reaction conditions: **4** (0.1 mmol, 0.05 M in  $\text{CF}_3\text{CH}_2\text{OH}$ ) was added dropwise to a vial containing  $\text{NaBH}_4$  at 0 °C. The reaction was continued for 4 h min at 0 °C.

**Scheme 5.**

Synthesis of Enoxime with Ethoxide or Thiophenolate as Nucleophiles<sup>a</sup>

<sup>a</sup> Reaction conditions. NaOEt as the nucleophile: **4** (0.1 mmol, 0.05 M in CH<sub>3</sub>CH<sub>2</sub>OH) was added in a vial containing CH<sub>3</sub>CH<sub>2</sub>ONa (1.2 equiv., 0.1 M in CH<sub>3</sub>CH<sub>2</sub>OH) dropwise at rt. The reaction was continued for 2 h at rt. RSH as the nucleophile: **4a** (0.1 mmol, 0.05 M in CH<sub>2</sub>Cl<sub>2</sub>) was added in a vial containing RSH (1.2 equiv. 0.1 M in CH<sub>2</sub>Cl<sub>2</sub>) and triethyl amine (2.0/3.0 equiv.) dropwise at rt. The reaction was continued for 1–2 h at rt.